

Current challenges and potential directions towards precision microscale additive manufacturing – Part I: Direct ink writing/jetting processes

Dipankar Behera, Michael Cullinan *

Nanoscale Design and Manufacturing Laboratory, J. Mike Walker Department of Mechanical Engineering, The University of Texas at Austin, Austin, TX, USA

ARTICLE INFO

Keywords:

Aerosol jet printing
Microscale Additive manufacturing
Electrohydrodynamic printing
Direct ink writing
3D printing
Binder jetting

ABSTRACT

This paper is the first in a series of articles which comprehensively discuss the state-of-the-art in microscale additive manufacturing processes and present solutions to challenges impeding their scalability. In this paper, a class of additive manufacturing techniques known as Direct Ink Write/Jet Processes are explored which have been used by researchers for fabrication of microscale parts with varying geometric freedom. The paper identified the key challenges to high throughput 3D microfabrication using these processes, by analyzing the material constraints, geometric constraints, feature-size resolution limits and throughput limits. While some of these challenges can be overcome by novel precision engineering approaches, there are several others which need an acute understanding of material systems, process parameters and critical components. This paper identifies these challenges and suggests potential approaches to eliminate them with the goal of fabricating true-3D parts at high throughputs.

1. Introduction

Microscale additive manufacturing has gained extensive attention over the past two decades for its ability to fabricate complex microscale products with applications in semiconductor, medical devices and energy sectors. The primary motivation behind exploring these process techniques is the design independence afforded by additive manufacturing in general. However, there are several challenges associated with developing microscale AM processes which hinder the scalability and production-scale adoption of these processes. This paper is the first of a four-part series of articles which discuss different processes categorized by their governing process physics. Part I of this series (this paper), discusses several Direct Ink Writing/Jetting processes which have been adapted to fabricate microscale parts. Direct writing (DW) is an umbrella term for a class of additive manufacturing technologies which involve the transfer, conformal deposition, and consolidation of material onto a substrate in a preset pattern. From a microscale AM perspective, the method used in material delivery and bed consolidation techniques can be used to classify DW processes into four main sub-categories – Extrusion-based (Flow-based Direct Ink Write or F-DIW), Droplet-based (Aerosol jet, Electrohydrodynamic Jet and Binder Jetting), Laser-based (LCVD, LIFT), and Tip-based (Dip-pen Nanolithography) [1–3]. In this paper, we have focused on liquid

deposition dominant DW processes which include extrusion-based and droplet-based techniques. The paper explores the challenges associated with the application of flow-based direct write processes to fabricate true-3D parts. Further, the physical limitations to the scalability of these processes have been discussed and potential solutions/improvements have been proposed. Part II of this paper series will focus on laser-based trapping, curing and heating processes while Part III of this series will focus on energy induced deposition and hybrid electrochemical processes and Part IV will discuss the future perspective of microscale additive manufacturing.

Overall, in this series of papers we will evaluate each of the microscale AM techniques based on four main criteria – range of processable materials, feature-size resolution, degree of geometric freedom, and process throughput. The general objective of these articles is to help develop a comprehensive understanding of the current capabilities and limitations of various microscale additive manufacturing processes. The papers outline the current status of the technology and presents discussions on the limiting factors to scalability of these processes. Furthermore, they also highlights the potential approaches that have been implemented in the literature to address these challenges and explores several auxiliary and complementary ideas to overcome the process limitations and enhance precision manufacturing. Based on these ideas, general guidelines and design principles are discussed to

* Corresponding author.

E-mail address: michael.cullinan@austin.utexas.edu (M. Cullinan).

drive the integration of microscale AM processes in high-throughput production environments.

2. Flow-based direct ink write

2.1. Description of flow-based direct ink write process

Flow-based direct ink write (F-DIW) processes are characterized by a continuous flow of liquid through a capillary tip or nozzle induced by the direct application of constant displacement or constant pressure to the liquid [1,4]. Constant displacement techniques use a plunger or an extruder to form continuous filaments of liquid which are deposited on to the substrate at uniform volumetric flow rates. Constant pressure techniques apply a uniform pressure to a liquid reservoir to produce the same continuous filaments, however, minor rheological changes during operation can significantly affect print quality. In F-DIW relative translation between the ink nozzle and substrate is used to generate the desired pattern. A wide variety of ink materials and compositions have been used to fabricate 3D parts with F-DIW. The development of highly specialized inks has been of interest as precisely controlled ink flow and deposited structure mechanical properties are critical for F-DIW. Inks with cores (low-stress regions) for shape-retention and support capabilities, and shells (high-stress regions) which promote interlayer fusion and a boundary slip region [1,3]. These inks can be further solidified or consolidated by solvent-evaporation [5], material gelation [4,6], and temperature-induced phase change [7,8] to form 3D parts. FDIW techniques and its variants have been used to fabricate microvascular networks with minimum resolution of 100 μm , sub-5 μm resolution micro-periodic structures, and interdigitated micro-batteries with a 30 μm nozzle, etc. Fig. 1 shows a detailed schematic of FDIW and presents some of the parts that have been fabricated using the process.

2.2. Materials

2.2.1. Materials capabilities and challenges in F-DIW

Metallic, ceramic, and polymer inks have been used in fabricating microscale structures with F-DIW [1,11,12]. However, to achieve desired part specifications, the inks used must be tailored to have specific rheological and solidification characteristics. Ideal F-DIW inks need to exhibit a shear thinning behavior and maintain a constant cross section after exiting the nozzle so that they can achieve structural rigidity after deposition [1]. In general, inks used for F-DIW can be categorized into either colloidal aqueous gels or colloid-based thermoplastic polymers [1,4]. For fabricating high-resolution microscale parts, the particle sizes in these inks should be an order-of-magnitude smaller than the part resolution. The inks contain precursors in the form of micro/nano-scale powders, organic material, surfactants, dispersants, and binders etc [3]. An important property of the materials used for F-DIW is that they should be able to flow through the nozzle and form a continuous filament upon exit with consistent cross-sectional area, and dry upon contact with the substrate to retain the shape and form the layer. The primary challenges in engineering materials for F-DIW are ensuring a high-density part and avoiding nozzle clogging issues in high resolution parts. For example, the theoretical packing density of FCC and HCP structures with monodispersed spherical particles is around 74%, which means that there would be at least 26% voids in the resulting structure. This implies that the dielectric constant of the microproduct will be an order of magnitude lower, according to the logarithmic rule of mixture for dielectrics [3]. This introduces the need to design materials and inks which can have lower porosities after deposition, drying and sintering. Therefore, the material rheology, particle size and morphology, particle distribution, wetting characteristics, thermal characteristics, and substrate properties must be optimized for desired performance [1,3].

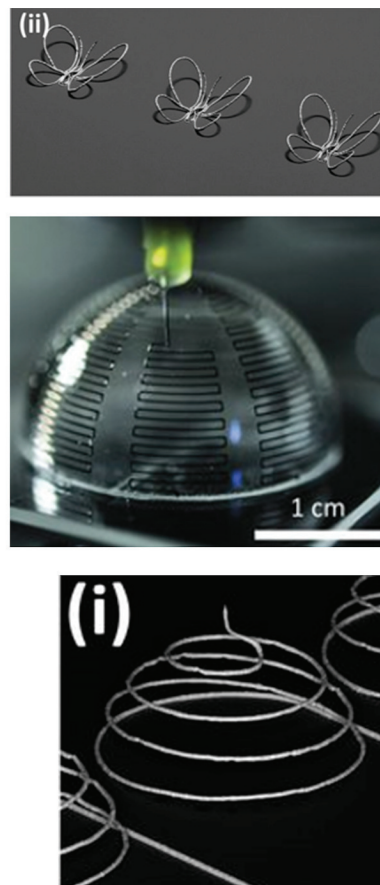
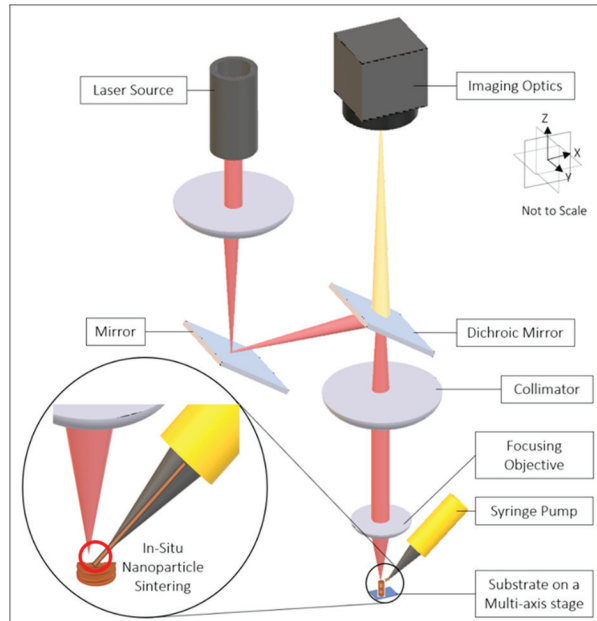


Fig. 1. (a) Schematic of the Laser-assisted Flow Direct Ink Write (FDIW) process based on the work by Skylar-Scott et al. [9]. Ag Nanoparticle ink is pushed through a small diameter nozzle using a constant pressure or constant displacement pump. The FDIW approach shown here uses a laser in-situ to sinter the Ag NP ink and create freestanding 3D structures. The optical subsystems are used for focusing the laser onto a 100 μm spot and enable process monitoring and control. (b) Printed and sintered freestanding butterflies [9] (Reproduced with permission from PNAS) (c) Optical image of antenna being conformally printed on a hemispherical surface using an FDIW setup [10] (Reproduced with permission from Advanced Materials) (d) Hemispherical spiral array printed using laser-assisted FDIW [9] (Reproduced with permission from PNAS).

2.2.2. Possible approaches to overcome materials challenges for F-DIW

The porosity of fabricated parts can be controlled with the introduction of poly-dispersed inks with bimodal particle size distributions engineered such that nanoparticles can fill the spaces caused by inefficiencies due to the packing factor of the microscale particles. However, this architecture introduces additional challenges associated with processing nanoparticles to avoid issues related to oxidation and particle agglomeration. Inks with higher particle loadings lead to an increase in operational pressures and clogging in the nozzle. While there are some theoretical and numerical frameworks to design nozzles to maximize anti-fouling performance, experimental studies suggest that nozzle clogging in F-DIW is predominant when $D_N/d_p \sim 150$ where D_N is the diameter of the nozzle and d_p is the diameter of the largest particle present [13]. Additionally, despite being a complex process, chemically treating the nozzle can also improve the flow characteristics of the liquid.

A passive deposition method was suggested by Smay et al. [14], which avoided nozzle clogging by decoupling the deposition and drying process. Colloid-based-gels and nanoparticle gels were deposited in an oil with poor wettability that suppressed drying and facilitated sub-100 μm features. The shape was maintained by purging the oil and subsequent drying of the part. In general, the transition from a concentrated colloid to a colloid-based-gel is activated by introducing a change in pH or ionic concentration in the system. The deposition quality is governed by the relationship between colloid volume fraction and the elastic properties of the liquid [1,3,13].

$$y = k \left(\frac{\phi}{\phi_{\text{gel}}} - 1 \right)^n \quad (2.2)$$

where y is the shear yield stress or elastic modulus, k is the constant, ϕ is the colloid volume fraction, ϕ_{gel} is the desired volume fraction after gelation and n is the scaling factor. This general approach has been effective for fabricating a wide range of ceramic materials including silica, barium titanate, silicon nitride, and hydroxyapatite etc [1]. Designing inks with predetermined performance characteristics before and after the deposition, and equally as important, after post-processing, is crucial for the development of future F-DIW materials.

2.3. 3D feature fabrication

2.3.1. Capabilities and challenges for fabricating 3D features

In F-DIW a nozzle lays down a continuous volume of material which can be stacked in a layer-by-layer manner to produce a 3D structure. The layer thickness is primarily dependent on the diameter of the nozzle tip. In principle, space-filling solids, hierarchical structures with high aspect ratio features, true-3D cantilevered and angled structures can be fabricated using the process. Some variants of the F-DIW process are better suited for fabricating 2D features conformally on contoured surfaces [10]. However, for solid freeform designs, it is important that the liquid can flow into interstitial gaps within the fabricated structure to avoid a highly porous final part [1]. On the contrary, for hierarchical structures, it is important that the bottom layers act as support material for the subsequent layers. Fabricating angled or cantilevered structures is very difficult for the F-DIW process without using sacrificial support structures or appropriate material consolidation. Additionally, like other direct write processes, the critical challenges for F-DIW lie in optimizing the tool path for layer-by-layer stacking and reducing the number of toolpaths to avoid intermittent flow operation.

2.3.2. Possible approaches to overcome 3D feature fabrication challenges for F-DIW

While out-of-plane structures without any support material can be printed using F-DIW, the print characteristics depend heavily on the performance of the stiff core and compliant shell of the material extruded. However, using in-situ laser treatment of the material exiting

the nozzle, Skylar-scott et al. [9] were able to fabricate more complex, high-resolution freestanding structures like helical springs using 85% loaded Ag nanoparticle ink (as shown in Fig. 1d). In addition to a precise control of the position of the nozzle and the laser head, it is critical to identify the minimum distance between the nozzle and the laser to avoid upstream heat conduction in the liquid and eventual clogging of the nozzle. By using a pulsed laser the overall heat transfer to the upstream ink and substrate was limited while effective heating of the nanoparticles in the extruded ink was maintained. Additionally, a freeze-drying approach was used for liquid metal alloys to fabricate freestanding structures using F-DIW process. As the liquid metal (Eutectic composition of Gallium and Indium) exits the nozzle, an elastic layer of gallium oxide maintains the structural integrity [15]. As the extruded filament touches the cold substrate, the freeze front propagates through the structure to increase its structural stability. Gannarapu et al. [16] developed a model to predict the freeze front propagation through the conductive and convective heat transfer and phase-change mechanisms, which could be crucial in designing to avoid nozzle clogging issues for high resolution structures. These freestanding structures are further encapsulated in thermoset elastomers for flexible electronics applications [15,16]. However, the range of materials (liquid metal alloys) and applications for structures fabricated using this technique is quite narrow.

2.4. Feature size resolution

2.4.1. Feature size resolution capabilities and challenges

The resolution of F-DIW, unlike other direct write processes such as Aerosol-Jet printing and Electrohydrodynamic printing is significantly more dependent on the nozzle diameter [1,2,17,18]. In practice, only circular cross-sectional areas can be printed at minimum resolution because of the limitations associated with manufacturing nozzles with different shapes. While sub-100 nm quartz nozzles have been manufactured by uniformly pulling and shearing a heated capillary or etching into a Si substrate, the decrease in nozzle diameter necessitates a large increase in the pressure needed to displace high viscosity fluids, thereby decreasing process throughput. It can also lead to additional nozzle clogging and shearing issues, effectively limiting the operating window. While sub-10 μm resolutions have been regularly reported for F-DIW process, Skylar-scott et al. were able to repeatedly print 600 nm structures using a 1 μm nozzle diameter [9].

2.4.2. Possible approaches to overcome resolution challenges in F-DIW

As discussed in section 2.2.2, nozzle size and clogging restrictions have been empirically determined to occur when $D_N/d_p < 150$ where D_N is the diameter of the nozzle and d_p is the diameter of the largest particle present [13]. Based on this, further optimization of the process and material parameters could be done to identify printing windows for high resolution microparts. Additionally, discrete numerical studies from other manufacturing industries (such as continuous steel casting [19]) can be used as a framework to study the nozzle clogging issues that arise in sub-10 μm nozzles followed by comprehensive experimental validation.

2.5. Throughput

2.5.1. Process throughput capabilities and challenges

The highest reported volumetric throughput of the F-DIW process is $\sim 0.01 \text{ mm}^3/\text{h}$ at a 20 μm resolution in laser-DIW [9]. The process throughput is primarily limited by the speed of extrusion and deposition, and single nozzle and thus serial-write designs. For a high-resolution part made of high viscosity ink the flow rate would be lower for a constant pressure differential, effectively lowering the volumetric throughput of the process as the part resolution increases. The structural integrity and porosity of the final part may also be lower with use of lower ink viscosity or solids loading further limiting the scalability of the

F-DIW process.

2.5.2. Possible approaches to overcome throughput challenges in F-DIW printing

Novel multi-nozzle printhead designs have been explored to improve the overall throughput of the F-DIW process. Hansen et al. [20] fabricated a dual multi-nozzle printhead with microvascular networks in series using PMMA microfluidic channels. Although the print resolutions were lower, the throughput was orders of magnitude higher than the highest reported single-nozzle throughput. Independent multiple nozzle assemblies have also been explored by researchers to increase the throughput as well as allow multi-material fabrication capabilities. Lewis and group [21] fabricated capacitive soft-strain sensors for health sensing applications using an elastomer and an ionic liquid. Using multiple cores separated coaxially in the printhead, the group was able to achieve a 10x improvement in the fabrication speed. However, the integration, flow control and precision deposition challenges associated with sub-10 μm multi-nozzle printhead designs must be addressed to improve the throughput of the system.

2.6. Prognoses

The design and integration simplicity of the F-DIW process adds significant value to the potential adoption of the process for several microelectronics, MEMS and biomedical applications. While most of challenges associated with the process involve designing inks with the requisite properties, the process can be streamlined using novel deposition approaches and developing prediction algorithms for understanding the deposition dynamics. Using in-situ drying and annealing techniques, the F-DIW process can be extended to a variety of materials including metal nanoparticle inks. Furthermore, the overall throughput of the process can be increased by orders of magnitude by introducing multi-nozzle configurations with innovative algorithms for tool-path optimization.

3. Electrohydrodynamic (EHD) printing

3.1. Description of the EHD printing process

Spray-based printing processes can pattern functional materials over a wide range of substrates in a maskless manner, fabricate 2.5-3D structures and offer multi-material integration capabilities [22]. With significant advantages over subtractive microfabrication techniques like optical lithography, spray-based processes such as inkjet printing have

been used to additively fabricate multimaterial 3D mm-scale structures [23–25]. However, the resolution of inkjet printing is limited to $\sim 20 \mu\text{m}$, as the actuation pressures become impractically high with the decrease in nozzle diameter and increase in fluid viscosity required to increase resolution [26–28]. In contrast, electrohydrodynamic (EHD) printing can eject submicron resolution droplets, which makes it a viable alternative for micro/nano-scale additive manufacturing. In EHD printing, an electric field is applied at the nozzle tip, across the air gap and surface of the liquid containing conductive ions, to mobilize the ions at the liquid-air interface. The magnitude and polarity of the electric field can induce several different types of ejection modes. For microfabrication applications, an axially stable ejection mode like microdripping is typically used [29,30]. In the microdripping mode, a conical meniscus (Taylor cone) is formed at the tip of the nozzle which undergoes deformation as the electrical shear stress is increased. With a strong electric potential at the tip (100–1000 V), the electrical shear overcomes the viscoelastic force to eject pulsed droplets on to an electrically grounded substrate. The droplet sizes are an order of magnitude smaller than the nozzle diameter for stable modes. Another mode of operation, where a thin jet is formed after the deformation of the Taylor cone, has been applied to the fabrication of microscale 3D scaffolds [31]. Fig. 2 shows a detailed schematic of the EHD printing process. While EHD printing is primarily a deposition process, using phase change materials and applying bed consolidation techniques (like a sintering and curing) can adapt it to a more classical layer-by-layer AM process.

3.2. Materials

3.2.1. Materials capabilities and challenges

The materials for EHD printing need to be in liquid phase and must be engineered for good electrohydrodynamic behavior through addition of surfactants and electrically conductive particles. While a wide variety of liquid phase materials in solution, suspension, or even molten form can be printed using this process, avoiding agglomeration of suspended particles is key to achieving high resolution EHD printing. Additionally, the resolution and fidelity of the EHD printing process largely depends on fluid rheological properties like viscosity, surface tension and density, as well as electrical properties like conductivity and polarity (dipole moment).

EHD printing has been used to deposit metallic, carbon-based [28, 33], ceramic [30], and polymer-based conductive materials [31], semiconducting nanoparticles (quantum dots) [34], biomaterials [35] and molten metals [36] on a wide range of substrates. The primary materials challenges associated with EHD include particle-substrate interaction

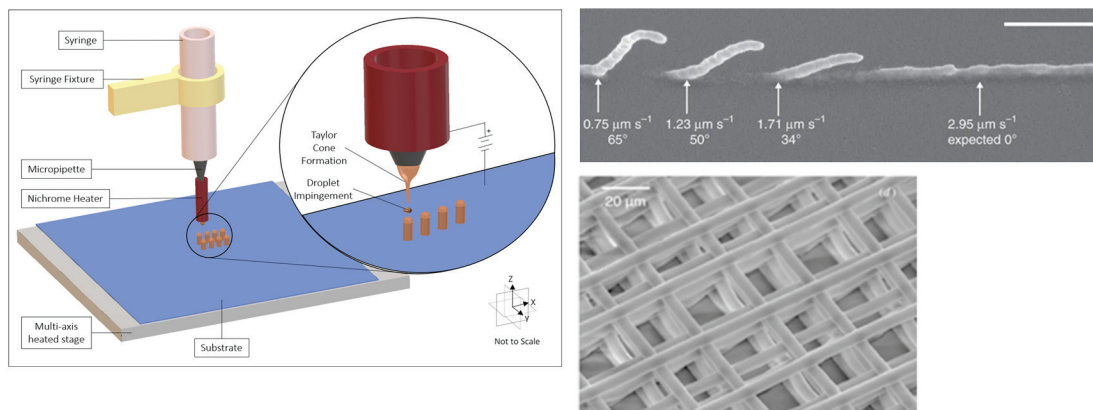


Fig. 2. (a) Schematic representation of the Electrohydrodynamic (EHD) printing. In EHD printing, an electric field is applied at the nozzle tip, across the air gap and surface of the liquid containing conductive ions, to mobilize the ions at the liquid-air interface. The magnitude and polarity of the electric field can induce several different types of ejection modes. The figure shows microdripping mode which is typically used for microfabrication purposes. (b) An optical microscope image showing the tilted freestanding (true-3D) nanodroplets using EHD printing process [32] (Reproduced with permission from Nature Communications). (c) 3D polymeric scaffolds fabricated using Electrohydrodynamic jet plotting [31] (Reproduced with permission from Journal of Micromechanics and Microengineering).

and wetting behavior, particle agglomeration, electrostatic charge accumulation during layer-by-layer printing, and poor solvent evaporation characteristics. It must be noted that these material challenges additionally limit the resolution, true-3D fabrication capabilities, and throughput of the process.

3.2.2. Possible approaches to overcome materials challenges for EHD printing

To achieve precise control of liquid extraction and deposition, the nozzle must be chemically coated with hydrophobic agents to avoid wetting beyond the confined capillary. The wettability of the liquid and the substrate is critical for 3D fabrication capabilities since a higher wettability (low contact angle) leads to faster evaporation of the solvent after the droplet lands on the substrate. Although the print resolution of EHD printing higher than inkjet printing, there is still an effective trade-off between particle concentration and resolution due to possible nozzle clogging. For metal NP inks, a typical concentration of 0.1–10 wt% has been successfully used in EHD printing to avoid clogging [17,22]. A higher concentration ink can also reduce the resolution as more nanoparticles would be deposited under the same conditions. Conversely, a higher solvent concentration might increase fabrication time for 3D parts in a layer-by-layer manner. Therefore, the materials used for EHD printing need to be highly customized in nature where the properties are dictated by other process limitations, which have been discussed in sections 3.3–3.5.

3.3. 3D feature fabrication

3.3.1. Capabilities and challenges for fabricating 3D features

The EHD printing process can fabricate high aspect ratio (~8:1) 3D materials using phase change materials like paraffin wax [29,37]. Researchers have also leveraged the continuous jetting mode for fabricating 3D scaffolds in an extrusion-style process. The droplet-on-demand printing mode can potentially fabricate closed 3D structures. However, the major limitations to fabricating 3D geometries using EHD printing are associated with the standoff distance between nozzle and substrate, droplet charge accumulation, and inherent design and process challenges associated with in-situ drying of the solvent. As the nozzle-substrate distance increases with the fabrication of high aspect ratio 3D structures, the electric potential between the nozzle and substrate must be increased to maintain a stable printing. Further, the printing fidelity is also affected by the electric field distribution for fabricating complex geometries using different printing and substrate materials. Droplet charge accumulation on non-conductive substrates can further affect the printing stability and hinder the fabrication of 3D structures. Hence, predicting printing behavior for 3D fabrication using EHD printing is challenging. Additionally, the droplet deposition technique can make it difficult to fabricate true-3D overhanging structures without effectively removing excess solvents and consolidating the previous layers. While an intermediate curing or sintering step can be implemented in line with layer-by-layer deposition, it can drastically affect the process throughput and reduce part quality. Furthermore, printing curved features is a challenge as it would involve electrostatically deflecting the jet and controlling the deflection to obtain the desired radii of curvature.

3.3.2. Possible approaches to overcome 3D feature fabrication challenges for EHD printing

The tradeoff between standoff height and electric potential is an active area of research to enable EHD printing on non-conductive surfaces and improve the process conformality on distorted surfaces with varying standoff heights. A commonly explored approach is to design a printhead that couples the ground electrode and the nozzle by adding a sub-25 μm inner diameter ring shaped gated electrode between the nozzle and substrate [22,28,33,38,39]. However, the scalability of this approach for sub-25 μm droplet sizes presents several challenges

including clogging of the gated plate due to the strong radiating force emanating from the grounded electrode [40]. To counter this effect, Tse and Barton introduced a dual electrode layer field shaping printhead design to mitigate the effect of the radiating forces around the nozzle, while maintaining print resolution below 10 μm [40]. Another design presented by Barton's group used subsonic airflow to direct the trajectory of the droplets on to a tilted surface with height variations and demonstrated sub-20 μm repeatable printing resolutions [41]. The effect of the charge accumulation for printing high density 3D structures can be mitigated by using a conductive substrate, or by continually reversing the polarity of incoming droplets to neutralize residual charge. Integrating these design iterations with the conventional EHD printing process can potentially improve the dimensionality of the process as standoff heights can be increased and the high-resolution droplets can be printed on to tilted surfaces. Liashenko et al. presented an EHD printer operating in jetting mode allowing for a precise deflection of the jet to obtain curved stacked features [42].

While phase change inks have been used to demonstrate the 3D fabrication capabilities of EHD printing, for other functional materials it is critical that the previous layers are purged of excess solvent. Customized nanoparticle inks with minimal solvent have also been used to fabricate sub-100 nm pillar-like structures 3D structures. This can be achieved by designing inks with highly volatile solvents at STP which evaporate in flight. The autofocusing effect of EHD, where the initial droplets acts as a charged electrode under applied electric field to attract the incoming ones, can help to maintain the structural integrity of complex 3D designs. Galliker et al. presented high resolution true-3D structures at a slant angle of 66° (from vertical), using the autofocusing effect [32] as shown in Fig. 2b. The as-deposited structures can be further annealed to improve the thermal and mechanical properties. Additionally, in-situ drying and sintering/curing of the layers to remove solvents and consolidate the particles, respectively, can be implemented as an intermediary step for 3D EHD printing.

3.4. Feature size resolution

3.4.1. Feature size resolution capabilities and challenges

The minimum reported resolution of the EHD process is 50 nm³². A significant advantage of EHD printing compared to other AM processes is the ability to dispense submicron droplets of high viscosity liquids like polycaprolactone (PCL) [31]. However, it must be noted that there is a tradeoff between the resolution and nozzle size. If the nozzle size is reduced, the nanoparticle loading concentration must be reduced to avoid clogging the nozzle. As a result, for low viscosity inks with sub-10 nm particle sizes, it is possible that there are no nanoparticles present in any individual dispensed drop [32]. Additionally, the droplet stability must be taken into consideration as certain resolutions can be achieved with only certain given concentrations of nanoparticle suspension and electric field strengths. Furthermore, the droplet-style printing process without any nanoparticle consolidation can produce poorly shaped parts with high surface roughness. Although, process parameters for high resolution EHD printing have been experimentally optimized for different materials, there are still significant challenges for production scale integration of the process.

3.4.2. Possible approaches to overcome resolution challenges in EHD printing

The resolution of the droplets deposited by EHD printing is affected by process conditions like the voltage applied across the liquid, the flow rate, the fluid rheology, and the surface charge concentration at the nozzle tip. The substrate conductivity and temperature also affect the morphology of the deposited droplet. A higher resolution droplet can be achieved in the drop-on-demand EHD operation by increasing the applied voltage and reducing the volumetric flow rate. A commonly used strategy to decouple the impact of applied voltage on print resolution and frequency is by using a modulated pulsed voltage [43]. The

pulse frequency precisely controls the printing frequency and the pulse duration, duty cycle and baseline amplitude can affect the Taylor cone formation, droplet detachment, print resolution, and frequency. For pulsed EHD printing, the droplet diameter (resolution) scales as $(d_n * d_m)^{1/2}$ where d_n is the nozzle internal diameter and d_m is the jet diameter, under the assumptions that the nozzle is thin and the conductivity of the liquid is high ($>10^{-5}$ S/cm) [44]. However, strong experimental correlation is still required to optimize the process parameters for the EHD printing process, which is difficult to generalize because of the wide parameter space and large bounds. Therefore, researchers have sought out theoretical and mathematical modeling of the EHD printing process to understand the effect of different parameters during different stages of EHD printing, with models for Taylor cone formation, jet formation, droplet ejection, inflight mechanics and droplet settlement [22]. From an AM perspective, the autofocusing effect [32] and its impact on resolution of subsequent layers could be modeled using numerical and FEA techniques. As a result, future work is needed to significantly improve the resolution of multilayer parts and bring them in line with the resolutions that can be achieved in single layer EHD structures.

3.5. Throughput

3.5.1. Process throughput capabilities and challenges

A wide range of process throughputs have been reported for EHD printing depending on the material used and process requirements. Generally, the pulsation frequency which directly impacts the throughput scales according to equation (3.5)⁴⁴.

$$f \sim \frac{KE^2}{\epsilon\mu L} \sqrt{\frac{\rho d_n^5}{\gamma}} \quad (3.5)$$

where f is the pulsation frequency, K is the conductivity of the liquid, E is the electric field, ϵ is the dielectric constant of the liquid, μ is the viscosity of the liquid, L is the length of the nozzle, ρ is the density of the liquid, d_n is the inner nozzle diameter and γ is the surface tension of the liquid-air interface at the meniscus. However, these scaling laws provide only a qualitative basis for setting the process parameters, and further optimization must be done to improve the throughput of the process. Further the interaction between neighboring jets can lead to cross talk which deprecates the reproducibility of the print over a large range.

The throughput corresponding to sub-100 nm resolution is around 0.00036 mm³/h [17]. Conventional single nozzle designs and tradeoffs between resolution, material rheology, and process speed are the primary factors responsible for the low process throughput.

3.5.2. Possible approaches to overcome throughput challenges in EHD printing

Researchers have explored parallelizing the EHD process in order to improve throughput through the use of multiple independent nozzle designs integrated with field shaping printheads [45,46]. Ideally, the throughput should scale linearly with the introduction of multiple nozzles. However, printing stability was affected due to the electric field distortions at the printheads making the throughput scaling significantly less than linear [45]. Electric field simulations of the multi-nozzle configurations are a useful tool in determining the field distribution at varying potentials to avoid any “cross-talk” issues but don’t solve the fundamental problem. Choi et al. and group successfully have simulated multinozzle configurations to minimize the cross-talk between electrodes and improve the print fidelity [47,48]. Precise positioning and control of the nozzles is also critical for good overlay registration and print stability and can be achieved by using nanopositioning mechanisms along with vision-based techniques for feedback control and process monitoring.

3.6. Prognoses

The high-resolution multi-material printing capabilities of EHD printing make it a promising technique for micro/nano-scale AM applications. Conversely, there are significant scalability challenges associated with the process in fabricating near-net shaped parts with a high throughput. Integrating novel approaches to address the key challenges associated with the process can potentially improve the printing stability, multimaterial integration, 3D fabrication capabilities, but throughput will likely always be a problem. Therefore, the greatest potential for EHD could be its integrated with other higher throughput but lower resolution, microscale AM processes to fabricate high-resolution features, which might potentially improve the overall throughput of manufacturing of complex 3D microparts.

4. Binder jetting process

4.1. Description of the binder jetting process

The Binder Jetting (BJ) process (also known as Three-Dimensional Printing or 3DP™) was developed in the early 1990s at MIT by Cima and Sachs [49,50]. Since then, the technology has been primarily licensed to several companies based on the materials being processed. Like other powder-based processes, the base material is uniformly spread on the bed. However, instead of using some form of energy for powder bed consolidation, the BJ process uses selectively deposited liquid-phase binder to hold the powder material together. During the evaporation of the liquid material, there is redistribution and deposition of suspended particles at the necking points in the as-deposited beds. The coating and jetting processes are repeated for every layer until the part is formed. The binder material promotes the adhesion between the particle layers as well. The resulting material system, also known as the ‘green part’, is separated from the surrounding loose powder using water immersion or jetting. The green part, however, must undergo energy-based consolidation to improve the physical characteristics of the final part. Fig. 3 shows the general schematic of the binder jetting process. It must be noted that usually the green part is developed and then sintered separately, but some approaches use an in-situ heater to cure/sinter the green part, like selective laser sintering/melting processes.

4.2. Materials

4.2.1. Materials capabilities and challenges

The key material systems for the binder jetting process are the raw powder (polymers, metals and ceramics), binder and additives. While the powder sets the structural foundation for the part which is being fabricated, the binder is used to selectively pattern each layer of powder to achieve the end design. Additives are primarily used with the raw powder to improve the physical properties and part porosity [51]. Material depositability is critical in determining the overall efficiency of the process. The mobility of the particles in either dry or wet form is also dependent on the powder bed particle shape. While spherical particles provide better mobility than faceted/anisotropic particles due to lower interparticle friction, the packing density of the latter may be higher. Commonly used dry deposition methods include counter-rotating rollers for spreading the powder bed, fluidized beds, doctor blade configurations, and vibration to assist powder flow. As smaller particles tend to agglomerate and affect the uniformity of the bed, powder particles with sizes lower than 20 μm are deposited in a slurry form, using doctor blade coating and slip casting [51,52]. The solvent/carrier material is then removed using a drying process which effectively adds to the deposition times. Additives can be incorporated with the powder material to improve depositability, part characteristics, dimensional stability and part porosity.

The binders form an important aspect of the material selection

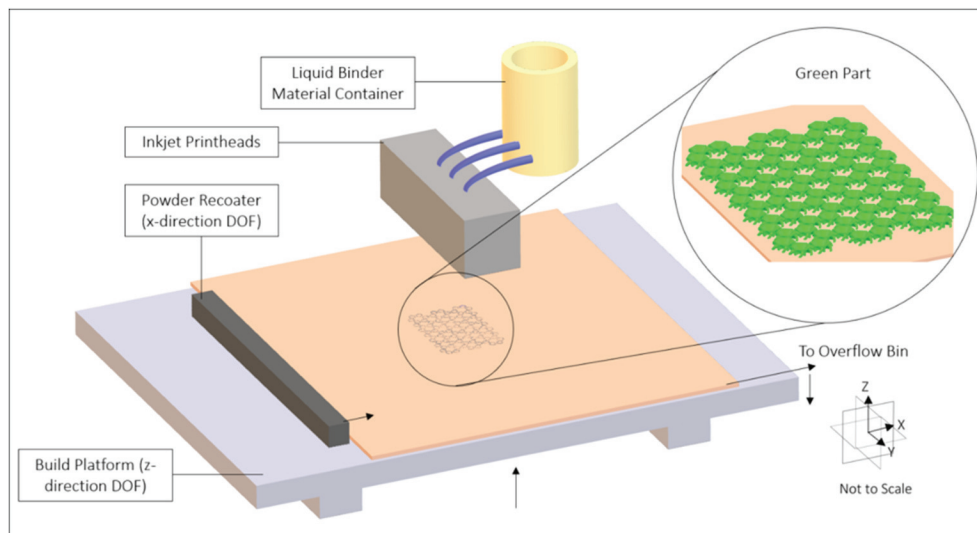


Fig. 3. Schematic of the Binder Jetting process. A powder recoater is used to spread the powder uniformly on the powder bed. The liquid binder is inkjetted selectively in the regions on the powder bed which need to be consolidated. After the first layer is completely jetted, the next layer is coated and bound using the binder liquid and the process is repeated to form a 3D part.

process for the BJ method as they consolidate the powder into the initial green part. The combination of binder and powder determines the robustness and versatility of the resulting fabricated structure. A commonly used classification criterion for the binder material are based on the binding location and the binding methodology [51]. There are two main binder types based on the binding location– in-liquid and in-bed. An in-liquid binder contains the necessary binding elements within the jetted liquid while an in-bed binder is a material added with the powder bed. In-liquid binders are usually compatible with a wider range of powders, but issues associated with liquid dispensing like nozzle clogging and uneven droplet formation are present in BJ. While this issue can be bypassed by blending a binding material like plaster to the base powder (in-bed binder), it involves an additional powder formulation step. Based on the binding methodology, binders are classified as organic/inorganic liquids, in-bed adhesives, metal salts, hydrating chemicals, phase-change materials, and acid/base systems etc [51,52]. Powder-binder compatibility is important for developing a stable printing regime, but it can also be considered as a limitation of the process since finding a reliable material combination requires thorough empirical exploration. Different powder and binder mixtures must be evaluated to understand absorption by the powder and the cohesivity of the green part specifically.

The versatility and cost of the binder jetting process makes it important to identify the physical limits associated with it. However, adapting binder jetting process for sub-10 μm additively manufactured parts involves several materials challenges, including development of new materials systems for fabricating true-3D green parts. The powder material, additives, and binder material sizes should be an order of magnitude lower than the feature-size resolution for reliable micro AM. This presents additional challenges for deposition of nanoparticle inks/slurries and binder materials.

4.2.2. Possible approaches to overcome materials challenges for binder jetting process

The potential material challenges associated with the binder jetting process can be addressed with the development of new material systems. The resolutions needed for microscale 3D parts require the use of nanoscale inks and binders, which are difficult to stabilize at STP. Thin layers of these inks can be deposited using precision pre-metered coating processes like slot die coating or doctor blade coating. The ink layers can be dried before the binding action such that they act as the support

structure for the subsequent layers to form the green part.

4.3. 3D feature fabrication

4.3.1. Capabilities and challenges for fabricating 3D features

True-3D green structures with the help of the powder bed as support material have been created using the binder jetting process. Nanoscale powders are used with larger particles to improve the over packing density of the green part by filling the gaps between larger particles with the nanoscale particles [53,54]. However, without any initial bed consolidation, the process must rely on the strength of the green part with the unbounded powder acting as the support material. Therefore, fabrication of freestanding structures is not possible using the binder jetting process. While the binding action of the powders is a viable alternative to avoid directed energy-based deposition and printing techniques, and the heat-transfer issues associated with them, there remains a considerable amount of dependence on the material properties. Consequently, it can be posited that the true-3D fabrication capabilities of the process are affected by the combination of powder and binder being used.

4.3.2. Possible approaches to overcome 3D fabrication challenges for binder jetting process

From the perspective of microscale AM, the binder jetting process can be continued without any necessary modification if highly stable nanoscale powders are used which limit agglomeration at STP. However, the use of liquid phase materials like nanoinks and nanopastes makes it difficult to satisfy the requirement for creating a near-net shape green part with the help of binders. While liquid binders are most commonly available, there is a fundamental problem with the displacement of particles from the design region due to the miscibility of the material and the binder. A potential solution is to use UV curable binders which aid in avoiding particle agglomeration. Selective regions of the material may be held together by the cured resin to form the green part, and additional sintering/annealing operations may create final microparts effectively gaining the resolution and design benefits of selective laser without the issue of heat affected zones. From a process design standpoint, there are no fundamental restrictions which may impede the fabrication of true-3D parts using binder jetting. Post-processing techniques like infiltration which uses capillary action to fill the voids in the final part after the binder is removed can also be used

to improve the strength of the final 3D part.

4.4. Feature size resolution

4.4.1. Feature size resolution capabilities and challenges

Commercially available binder jetting printers have been optimized to fabricate 20 μm feature microparts with 4 μm surface roughness [2]. The lateral and vertical resolution of the binder jetting process primarily depends on the particle size, size of the binder droplet, thickness of the layers being deposited, and accuracy of the mechanical scanning system. To achieve sub-10 μm features, a precise deposition method is needed in addition to a lower particle sizes by an order of magnitude. As mentioned in the previous sections, there are no precedents in the industry or research on using nanoscale powders to fabricate full-scale microproducts using the binder jetting process.

4.4.2. Possible approaches to overcome resolution challenges for binder jetting process

The binder material droplet size is usually larger than the powder particle size to promote effective adhesion at the powder and layer interfaces. The binder migration process, which involves identifying the intermediate states involved between the binder contacting the powder particles at the surface and reaching an equilibrium, plays a critical role in determining how much powder will be bound and in what shape. It is also important to characterize the velocity of binder deposition and the contact angle with the material as it determines the particle volume which can be bound. Additionally, the bed particle morphology and size distribution become critical factors in creating microscale parts. However, conventional nozzle-based techniques like inkjet printing are limited by the nozzle design and geometry. The droplet size may be reduced, and spraying modes can be controlled by applying a high electric field across the nozzle, a method which defines EHD printing technology. Recoating and redistribution of thin and uniform powder beds may be achieved using precision coating technique like slot die coating.

4.5. Throughput

4.5.1. Throughput capabilities and challenges

A significant advantage of binder jetting over other microscale AM processes is the speed. Commercially available binder jetting tools have speeds ranging from 166×10^3 mm [3]/hr to over 1600×10^3 mm [3]/hr [55] for a minimum layer height of 50 μm . The overall throughput improves with the increase in layer height. The throughput challenges associated with the process are derivatives of the challenges in reducing the resolution of the process. Another key limitation to the binder jetting throughput is the time it takes for the binder to spread which depends on the combination of powder and binder that must be used for the process. Miyajima et al. [56] studied the effect of printing speed on the quality of printed parts and observed that the dimensional accuracy of the printed samples reduces with an increase in the printed speed. Additionally, it must be noted that most binder jetting processes generate the green part which must be cleaned to remove unbound powder and sintered to achieve the required electromechanical properties.

4.5.2. Possible approaches to overcome throughput challenges for binder jetting process

The general approach to address throughput challenges in the binder jetting process is to identify the print window within which the dimensional tolerance of the green part is maintained. This can be achieved by better understanding of the liquid binder deposition, fluid-powder interaction, and permeation process through experimental and computational models.

4.6. Prognoses

Although binder jetting has been extensively researched in the literature because of the ease with which the system can be developed, creating microproducts with feature-size resolutions under 100 μm is difficult due to problems associated with powder and fluid particle size. At smaller scales, there is a high probability that the overall surface integrity of the green part would be significantly affected due to the potential agglomeration of powders. However, the technological readiness of this process qualifies it as an excellent alternative for fabricating larger features, and smaller features can be fabricated using other processes.

5. Aerosol Jet Printing process

5.1. Description of the aerosol jet process

The concept of aerosolization of bulk liquid to controllably deposit conformal patterns was developed as Maskless Mesoscale Material Deposition (M^3D) under DARPA's Mesoscopic Integrated Conformal Electronics (MICE) program [57,58]. AJP consists of 5 core processes – atomization, aerosol transport, collimation, focusing and impaction. First, the liquid to be deposited is atomized to 1–5 μm droplet size with ultrasonic or pneumatic atomizers. Then, the atomized droplets are transported to the deposition head by the carrier gas (also known as aerosol gas). Finally, the droplets are surrounded by an annular flow of sheath gas such that the material stream is collimated at the core of the deposition head exit nozzle. Towards the exit, the droplet velocities range can from 10 to 100 m/s at nozzle-to-substrate standoff distances of 1–5 mm. To maintain uniform deposition, the aerosol delivery process is continuous, and a shutter arm is used to block the flow. A precision XY-translation stage moves the substrate underneath the deposition nozzle to print the desired pattern. The primary application, and focus of research in AJP, is in flexible and hybrid printed electronics applications, where the patterns are mainly 2D or 2.5D⁵⁸. The ability of the process to achieve ~ 10 μm resolution for a wide range of materials makes it interesting for 3D microfabrication. However, it is important to develop a strong fundamental understanding the underlying physics in AJP to accomplish that. Fig. 4 shows the general schematic of the AJP process and some example parts fabricated using the method.

5.2. Materials

5.2.1. Materials capabilities and challenges in Aerosol Jet Printing

The AJP process is highly versatile because of the wide range of materials it encompasses. It has demonstrated printing of conductors (Ag, Au) [60,61], conductive polymers (P3HT, PQT) [62], single-walled carbon nanotubes (SWCNTs) [63], dielectrics (PMMA, Polyimides, BaTiO₃) [57], nanocomposites, and biomaterials. The AJP process can print liquids with a viscosity ranging from 1 to 2500 cP⁶⁴. The key considerations while selecting the right material for AJP applications are similar to other direct write (DW) processes. The material used in AJP process must be atomizable and monodispersed with minimal overspray, avoid nozzle clogging, have enough inertia for impaction, and have good substrate adhesion. Additionally, it must maintain near-bulk electrical characteristics after printing. From a practical standpoint, the selection of inks is usually an experimental process to identify the optimal parameters for good printing [65].

5.2.2. Possible approaches to overcome materials challenges for AJP

For effective aerosolization, the relationship between the atomizing technique (ultrasonic and pneumatic), and the rheological and morphological characteristics of the liquid (surface tension, viscosity, density) must be understood. While ultrasonic atomizer can produce highly uniform particles, it is restricted to very low viscosity (~ 20 cP) liquids. Conversely, pneumatic atomizers can process a wider range of

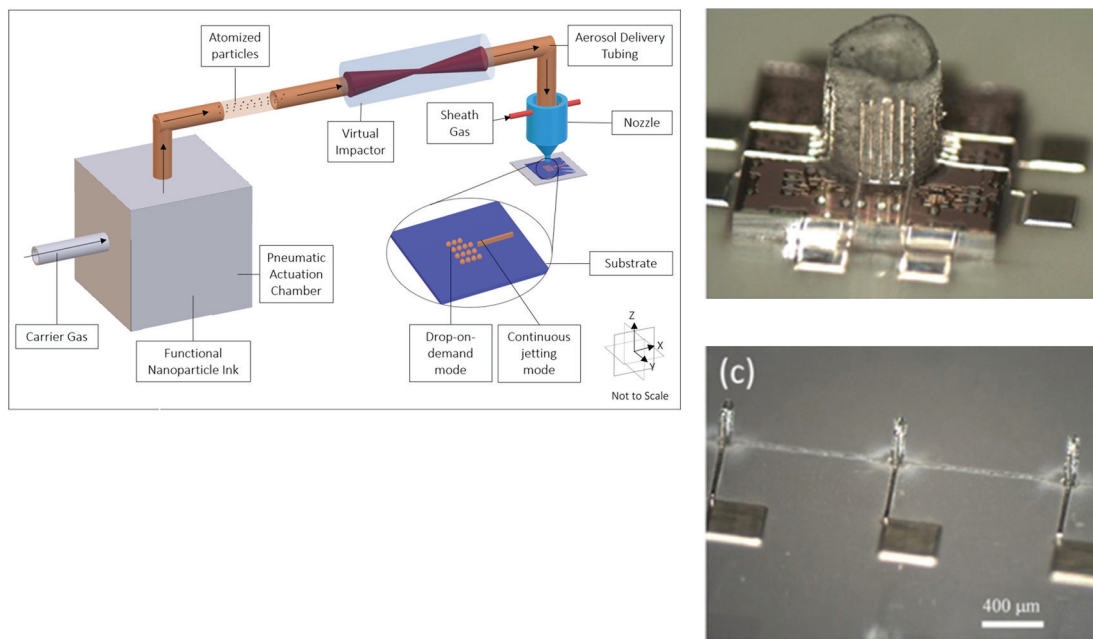


Fig. 4. (a) Schematic of the Aerosol Jet Printing (AJP) process. The AJP system consists of a reservoir with a pneumatic actuation mechanism that can aerosolize/atomize the functional ink into small parts. The atomized particles are transported into the deposition nozzle using the carrier gas and collimated to form a uniform cross section stream of particles using the sheath gas. (b) Conformally printed vertical lines on the walls of a dielectric pillar using AJP for microelectronics applications. The metallic interconnects are 22 μm in width [59] (Reproduced with permission from Ref. [59]. Copyright IOP Publishing Group). (c) 75 μm tall periodic dielectric pillars fabricated on top a Si wafer [59] (Reproduced with permission from Ref. [59]. Copyright IOP Publishing Group).

viscosities, but produce highly polydispersed streams, thereby requiring further process refinement. Uncontrolled evaporation of the ink during transport and deposition is another artifact of low viscosity AJP [66]. The high carrier velocities often lead to a loss of mass through evaporation of solvent during flight, that can reduce the inertia of the droplets and thereby affect their impact with the substrate [58,67,68]. A potential approach to addressing this was provided by Yang et al., where they introduced $\sim 10\%$ wt of low volatility solvent in addition to the primary solvent to avoid the complete drying of ink before impact [69]. A comprehensive understanding of the fluid rheological properties, contact angles, adhesion and drying is needed for better material integration with AJP process.

5.3. 3D feature fabrication

5.3.1. Capabilities and challenges for fabricating 3D features

The current capabilities of the AJP process are limited to 2D/2.5D fabrication, with several applications in mesoscale and microscale electronics. AJP has been used to fabricate passive electronics (resistors, capacitors, and inductors), interconnects, dielectric devices, interdigitated sensors, and waveguides [58,70,71]. The conformal nature of DW technologies has been widely explored for AJP. Commercial AJP processes are used for printing on conformal substrates to fabricate 3D antennas by changing the relative orientation between the printhead and the substrate [59,72] (See Fig. 4b). However, from a manufacturing perspective, this cannot be classified as a true-3D deposition approach, since the conformal substrate must act as a support structure for the deposited ink. Comparing with other micro-AM technologies which rely on support structures, either the support structures are fabricated using the process (like in an extrusion-based system) or the material acts as the support structure (Binder Jetting, μ -SLS, μ -SLA, TPL). While the conformal nature of the AJP process is convenient for several applications, the true-3D fabrication capability is difficult to achieve without in-situ material consolidation using an energy source. The layer-by-layer stacking of droplets traveling and impacting with high velocities can lead to splatter and potentially affect the overall stability and resolution

of the process.

5.3.2. Possible approaches to overcome 3D feature fabrication challenges for AJP

There is little evidence of fabrication of true-3D structures using AJP process. Saleh et al. [73] mimicked a naturally occurring crystal formation process to form the basis of the 3D fabrication of metal hierarchical structures using AJP. Using dropwise deposition, rapid solvent evaporation and solidification process, they were able to create a layer-by-layer true-3D structure. While the AJP process was the basic deposition method, controlled solidification of the droplets in a 90–110 $^{\circ}\text{C}$ temperature environment enabled creation of the part. To achieve better densification, the structure was sintered in an oven as part of the post-processing step [73]. While the structure was built without any support material or templating, it must be noted that the critical angle of growth was limited to $\sim 37^{\circ}$. The overall physical model relied on the evaporation parameters to achieve dry droplets before the subsequent layers could be deposited successively. This process demonstrates potentially integrating the capabilities of AJP with novel in-situ processing techniques to create true-3D parts. A similar approach can be used with UV curable materials like PDMS, and phase-change materials like wax, to obtain consolidated layers. However, the atomization and aerodynamic deposition of microscale droplets of wax may prove difficult. Furthermore, creating 90 $^{\circ}$ overhangs might not be possible without use of a sacrificial material as support structure.

5.4. Feature size resolution

5.4.1. Feature size resolution capabilities and challenges

Sub-50 μm [74,75] features have been consistently demonstrated with the help of AJP process. Unlike several DW processes, the generalized working principle of the AJP process does not depend on the particle size of the aerosol. While it is important to avoid polydispersity, the resolution of the process is affected by the nozzle diameter (d_n), aerosol stream diameter (d_a) and focusing ratio (FR) [66]. With simple assumptions like non-mixing volume displacement and parabolic, fully

developed laminar flow profile through a pipe, the focusing ratio can be calculated as shown in equation (5.4)⁷⁰.

$$\frac{d_a}{d_n} = \sqrt{1 - \sqrt{\frac{FR}{1 + FR}}} \quad (5.4)$$

where $FR = f_s/f_a$, and f_s and f_a are the sheath flow rate and aerosol flow rate, respectively. However, this equation loses validity for dry inks and higher flow rates [58,70]. During continuous printing using AJP, challenges such as poor edge quality, line discontinuity and overspray are common challenges in AJP [58,76]. Secor showed small droplets undergo rapid evaporation while interacting with the sheath gas, thereby affecting the material distribution in the aerosol beam thereby significantly degrading the print resolution over time [66,70,77]. This affects the reproducibility of the process as well. Additionally, the aerodynamic focusing approach, that is when the aerosol beam travels through a converging nozzle in the deposition head, also affects the resolution. An optimal way to enhance resolution is to force the droplets towards the center of the flow, away from the sheath gas streamlines. This can be achieved using an aerodynamic lens [78,79]. While larger droplets have higher inertia, and a greater tendency to be aerodynamically focused, a poorly design aerodynamic lens could lead to overfocusing. On the contrary, smaller particles with lesser inertia have a higher tendency to move with the gas flow streamlines, leading to a poor resolution, and potential splatters/overspray as discussed in Ref. [80]. The resolution can also be affected by an insufficient nozzle length, leading to undeveloped flow [70]. Fluid instabilities caused due to wet deposition of low viscosity inks can lead to line spreading which limits the resolution as well. This introduces a practical tradeoff between resolution and throughput for the system.

5.4.2. Possible approaches to overcome resolution challenges in AJP

There are several approaches that can be used for tackling resolution issues in AJP, especially from the perspective of aerodynamic focusing, impaction, and ink rheology. However, there are certain considerations which must be kept in mind while addressing these points. Aerodynamic focusing is needed when the resolution must be enhanced beyond the volume displacement effect of the sheath gas. This is where the particle-fluid coupling becomes critical, represented by the Stokes number (St). In a generalized system with thin-plate orifice assumptions for the exit nozzle, the best possible aerodynamic focusing can be achieved for a $St \sim 1$ [64,70]. The resolution improvement due to well-design aerodynamic lensing has been demonstrated by several researchers. Hoey et al. developed a converging-diverging-converging lens to achieve sub-5 μm resolutions [81,82]. Drawing on similar lines, sequential collimating and focusing of droplets with sufficiently high sheath gas to aerosol flow rate ratios could be useful in improving the resolution and achieving a stable flow. A better understanding of the process parameters which lead to overspray, line discontinuity and poor edge quality is also need. To that extent, Salary et al. developed a CFD model to track and verify the process parameters limits which would lead to these issues [76].

To tackle line spreading upon impact, a high sheath to aerosol flow rate ratio (≥ 2) and high print speed must be maintained, and smaller diameter nozzles must be used. With smaller nozzles, smaller particles with high inertia must be used, which might be a challenge since most of these approaches assume that there is no geometric aberration, the particle size distribution is good, and the initial droplets are centered around the sheath gas axis [70]. However, the Stokes number required for aerodynamic lensing is much higher than those for efficient impaction, so it can be assumed that designing with aerodynamic lenses is a much safer approach to achieve high resolution prints.

5.5. Throughput

5.5.1. Process throughput capabilities and challenges

The throughput of the commercial AJP tools range between 50 and 200 mm^3/h for 2D/2.5D applications [72,83]. The key parameters which affect the overall process throughput for a 2D AJP process are the aerosol flow rate and density. Additionally, when 3D fabrication considerations are made, the throughput will be affected by the intermediate steps needed to facilitate it. Rapid deposition of subsequent droplet streams might also lead to flow instabilities which can reduce the overall resolution of the system. While, most of the parameters affecting the throughput can be experimentally optimized, aerosol transport losses post atomization necessitates a more fundamental physical understanding [58,64,70]. Smaller particles, which are also critical for enhanced resolution, tend to stay off the axis of the flow if the flow rates are not sufficiently controlled, leading to poor focusing and overspray. In a more general sense, the particles away from the central axis have a higher tendency to impinge on the walls during transport, thereby reducing the volumetric throughput of the process. The material build-up on the walls might also lead to clogging of the deposition head, which is another process challenge. The fundamental physical mechanisms associated with these losses are due to gravitational settling and diffusion. While larger particles tend to settle under the force of gravity and hit the walls, smaller particles tend to get lost to diffusion. A longer aerosol delivery tube length will lead to a decrease in transport efficiency, but conversely, an insufficient length might lead to flow instabilities downstream due to undeveloped flows. Based on the work on gravitational settling by Thomas [84], the number of particles that remain suspended can be determined by equation 2.3.1.

$$P = 0.6366 \left(\alpha \beta + a \sin \beta - 2\alpha^3 \beta, \alpha = \left(\frac{3Lv_{TS}}{8v_a R} \right)^{1/3}, \beta = \sqrt{1 - \alpha^2} \right) \quad (5.5)$$

Where P is the probability distribution of number of suspended particles, L is the mist tube length, R is the radius of the tube, v_{TS} is the terminal settling velocity, and v_a is the average flow velocity. The volumetric throughput of the system depends on the aerosol flow rate, density and transport efficiency.

5.5.2. Possible approaches to overcome throughput challenges in AJP printing

The aerosol flow rate and density must be high to achieve an optimal throughput. If the viscosity of the ink is too high after impaction, it can lead to line spreading and splatter issues for subsequent prints and layers. Although a high flow rate and smaller nozzle can potentially enhance the resolution, it might decrease the overall deposition rate of the aerosol on the substrate. Therefore, an optimal process window must be identified which would also depend on the fluid rheology, atomization parameters, and desired feature resolution. Higher overall throughputs can be achieved fabricating continuous structures by parallelizing the process. Independent control of these nozzles can also create multiple designs on the same substrate simultaneously, as far as the process window is optimally defined. However, the multiple nozzle configurations could be primarily limited by space and geometric constraints.

5.6. Prognoses

The material capabilities, resolution, and throughput of the AJP printing process makes it unparalleled for microscale 2D printing of flexible and conformal microelectronics. Most of the research and application is concentrated on fabricating electronic interconnects, sensing devices, passive and active electronic components, and flexible circuits, which have several applications in semiconductor industry, hybrid electronics, microfluidics, and structural health monitoring.

However, the transition to true-3D fabrication space remains difficult without controlled removal of solvents or consolidation in previous layers before depositing the next layer. The overall throughput of the system would be reduced in a 3D fabrication regime, as additional time would be added due to the positioning and deposition of the subsequent layers, and the need for in-situ solvent removal. The trade-off between throughput and resolution will be critical for comparing the effective process windows that can be achieved with AJP process and other DW processes.

6. Conclusions

This article is the first in a four-part series of articles which investigate the challenges associated with microscale additive manufacturing processes. Part I presents the challenges associated with Direct Ink Writing/Jetting processes and possible approaches to address them. The key processes discussed in this section are Flow-based Direct Ink Write (F-DIW), Electrohydrodynamic Printing (EHD), Binder Jetting (BJP) and Aerosol Jet Printing (AJP). While FDIW can comfortably print 3D parts, high throughput fabrication of non-wire-like planar structures is difficult. Droplet-based deposition techniques like EHD, BJP and AJP are limited by the physics of droplet creation and deposition which determines the resolution and geometry of the parts. While there are approaches to improve the resolution of droplet deposition by altering the process parameters, there are tradeoffs associated with the throughput of the processes. While EHD can fabricate very high-resolution parts, achieving true-3D parts needs modeling and tuning material and process parameters to ensure layer-by-layer consolidation. Commercial AJP tools have been used for printed electronics applications and conformal printing, but it has similar challenges in fabricating 3D geometries. BJP can reliably fabricate true-3D parts, but freeform fabrication and sub-10 μm features is difficult due to the powder and binder morphology. A comparative analysis and comprehensive discussion of the general design guidelines that must be followed while developing these processes is presented in Part IV of this paper series [85].

Contributions

DB and MC have written, reviewed and edited all the sections.

Declaration of competing interest

The authors declare that they have no known competing financial interests or personal relationships that could have appeared to influence the work reported in this paper.

Acknowledgements

This series of publications is a joint effort by the members and affiliates of the Micro-Nano Technical Leadership Committee of the American Society for Precision Engineering (ASPE).

References

- [1] Lewis JA. Direct ink writing of 3D functional materials. *Adv Funct Mater* 2006;16:2193–204.
- [2] Vaezi M, Seitz H, Yang S. A review on 3D micro-additive manufacturing technologies. *Int J Adv Manuf Technol* 2013;67:1721–54.
- [3] Hon KKB, Li L, Hutchings IM. Direct writing technology — advances and developments. *CIRP Ann - Manuf Technol* 2008;57:601–20.
- [4] Lewis JA, Smay JE, Stuecker J, Cesarano J. Direct ink writing of three-dimensional ceramic structures. *J Am Ceram Soc* 2006;89:3599–609.
- [5] Tay BY, Edirisinghe MJ. Investigation of some phenomena occurring during continuous ink-jet printing of ceramics. *J Mater Res* 2001;16:373–84.
- [6] Smay JE, Iii JC, Lewis J. A. Colloidal inks for directed assembly of 3-D periodic structures. *Langmuir* 2002;84:5429–37.
- [7] Xu M, Gratson GM, Duoss EB, Shepherd F, Lewis JA. Biomimetic silicification of 3D polyamine-rich scaffolds assembled by direct ink writing. *Soft Matter* 2006;2:205–9.
- [8] Gratson GM, Lewis JA. Phase behavior and rheological properties of polyelectrolyte inks for direct-write assembly. *Langmuir* 2005;457–64. <https://doi.org/10.1021/la048228d>.
- [9] Skylar-Scott MA, Gunasekaran S, Lewis JA. Laser-assisted direct ink writing of planar and 3D metal architectures. *Proc Natl Acad Sci Unit States Am* 2016;113:6137–42.
- [10] Adams JJ, et al. Conformal printing of electrically small antennas on three-dimensional surfaces. *Adv Mater* 2011;23:1335–40.
- [11] Ahn BY, et al. Omnidirectional printing of flexible, stretchable, and spanning silver microelectrodes. *Science* (80-) 2018;323:1590–3.
- [12] Clendenning BSB, et al. Direct writing of patterned ceramics using electron-beam lithography and metallopolymer resists **. *Adv Mater* 2004;16:215–9.
- [13] Lewis JA, Gratson GM. Direct writing in three dimensions. *Mater Today* 2004;7:32–9.
- [14] Smay BJE, Gratson GM, Shepherd RF, Iii JC, Lewis JA. Directed colloidal assembly of 3D periodic structures. *Adv Mater* 2002;1279–83.
- [15] Ladd C, So J, Muth J, Dickey MD. 3D printing of free standing liquid metal microstructures. *Adv Mater* 2013;25:5081–5.
- [16] Gannarapu A, Dutta P, Gozen BA. International Journal of Heat and Mass Transfer Prediction of steady-state freeze front position during 3D printing of microstructures. *Int J Heat Mass Tran* 2017;115:743–53.
- [17] Hirt L, Reiser A, Spolenak R, Zambelli T. Additive manufacturing of metal structures at the micrometer scale. *Adv Mater* 2017;29.
- [18] Frazier WE. *Metal additive Manufacturing : a review*. vol. 23; 2014. p. 1917–28.
- [19] Barati H, Wu M, Kharicha A, Ludwig A. A transient model for nozzle clogging. *Powder Technol* 2018;329:181–98.
- [20] Hansen CJ, et al. High-throughput printing via microvascular multinozzle arrays. *Adv Mater* 2013;25:96–102.
- [21] Frutiger A, et al. Capacitive soft strain sensors via multicore – shell fiber printing. *Adv Mater* 2015;27:2440–6.
- [22] Han Y, Dong J. *Electrohydrodynamic printing for advanced micro/Nanomanufacturing : current progresses , opportunities , and challenges*. *J Micro-Nano-Manufacturing* 2019;6.
- [23] Calvert P. Inkjet printing for materials and devices. *Chem Mater* 2001;13:3299–305.
- [24] Ko SH, Chung J, Hotz N, Nam KH, Grigoropoulos CP. Metal nanoparticle direct inkjet printing for low-temperature 3D micro metal structure fabrication. *J Micromech Microeng* 2010;20.
- [25] Mehrali M, et al. A review on powder-based additive manufacturing for tissue engineering: selective laser sintering and inkjet 3D printing. *Sci Technol Adv Mater* 2015;16:033502.
- [26] Gao W, et al. The status, challenges, and future of additive manufacturing in engineering. *CAD Comput. Aided Des.* 2015;69:65–89.
- [27] Gao D, Yao D, Leist SK, Fei Y, Zhou. J. Mechanisms and modeling of electrohydrodynamic phenomena. *Int J Bioprint* 2018;5(1):1–19.
- [28] An BW, et al. High-resolution printing of 3D structures using an electrohydrodynamic inkjet with multiple functional inks. *Adv Mater* 2015:4322–8. <https://doi.org/10.1002/adma.201502092>.
- [29] Han Y, Wei C, Dong J. Super-resolution electrohydrodynamic (EHD) 3D printing of micro-structures using phase-change inks. *Manuf. Lett.* 2014;2:96–9.
- [30] Jayasinghe SN, Edirisinghe MJ, Wang DZ. Controlled deposition of nanoparticle clusters by electrohydrodynamic atomization. *Nanotechnology* 2004;15:1519–23.
- [31] Wei C, Dong J. Direct fabrication of high-resolution three-dimensional polymeric scaffolds using electrohydrodynamic hot jet plotting. *J Micromech Microeng* 2013;23.
- [32] Galliker P, et al. Direct printing of nanostructures by electrostatic autocrossing of ink nanodroplets. *Nat Commun* 2012;3:890–9.
- [33] Jeong YJ, et al. Direct patterning of conductive carbon nanotube/polystyrene sulfonate composites via electrohydrodynamic jet printing for use in organic field-effect transistors. *J Mater Chem C* 2016;4:4912–9.
- [34] Kim BH, et al. High-resolution patterns of quantum dots formed by electrohydrodynamic jet printing for light-emitting diodes. *Nano Lett* 2015;15:969–73.
- [35] Kim M, Yun HS, Kim GH. Electric-field assisted 3D-fibrous bioceramic-based scaffolds for bone tissue regeneration: fabrication, characterization, and in vitro cellular activities. *Sci Rep* 2017;7:1–13.
- [36] Han Y, Dong J. High-resolution direct printing of molten-metal using electrohydrodynamic jet plotting. *Manuf. Lett.* 2017;12:6–9.
- [37] Wei C, Dong J. Development and modeling of melt electrohydrodynamic-jet printing of phase-change inks for high-resolution additive manufacturing. *J Manuf Sci Eng* 2014;136:061010.
- [38] Lee S, An K, Son S, Choi, Satellite J. Spray suppression in electrohydrodynamic printing with a gated head. *Appl Phys Lett* 2015;103:133506.
- [39] Park JU, et al. High-resolution electrohydrodynamic jet printing. *Nat Mater* 2007;6:782–9.
- [40] Tse L, Barton K. A field shaping printhead for high-resolution electrohydrodynamic jet printing onto non-conductive and uneven surfaces. *Appl Phys Lett* 2014;104:143510.
- [41] Tse L, Barton K. Airflow assisted printhead for high-resolution electrohydrodynamic jet printing onto non-conductive and tilted surfaces. *Appl Phys Lett* 2015;107:1–6. 054103.
- [42] Liashenko I, Rosell-Llompert J, Cabot A. Ultrafast 3D printing with submicrometer features using electrostatic jet deflection. *Nat Commun* 2020;11:1–9.
- [43] Han Y, Dong J. Design , modeling and testing of integrated ring extractor for high resolution electrohydrodynamic (EHD) 3D printing. *J Micromech Microeng* 2017;27.

- [44] Chen C-H, Saville DA, Aksay IA. Scaling laws for pulsed electrohydrodynamic drop formation. *Appl Phys Lett* 2006;89:124103.
- [45] Pan Y, Huang Y, Guo L, Ding Y, Yina Z. Addressable multi-nozzle electrohydrodynamic jet printing with high consistency by multi-level voltage method. *AIP Adv* 2015;5: 047108.
- [46] Shigeta K, Industries T, Hoelzle D, Barton K. A multimaterial electrohydrodynamic jet (E-jet) printing system. *J Micromech Microeng* 2012;22(4):045008.
- [47] Choi KH, et al. Effects of nozzles array configuration on cross-talk in multi-nozzle electrohydrodynamic inkjet printing head. *J Electrostat* 2011;69:380–7.
- [48] Khan A, Rahman K, Hyun MT, Kim DS, Choi KH. Multi-nozzle electrohydrodynamic inkjet printing of silver colloidal solution for the fabrication of electrically functional microstructures. *Appl Phys A Mater Sci Process* 2011;104: 1113–20.
- [49] Sachs Emanuel M, Haggerty John S, Michael J, Cima PAW. Three-dimensional printing techniques. 1989.
- [50] Sachs Emanuel M, Cima Michael J, Williams Paul A, Brancazio D, Cornie J. Three dimensional Printing : rapid tooling and prototypes directly from a CAD model. *J. Eng. Ind.* 1992;114:481–8.
- [51] Utela B, Storti D, Anderson R, Ganter M. A review of process development steps for new material systems in three dimensional printing (3DP). *J Manuf Process* 2008; 10:96–104.
- [52] Utela BR, Storti D, Anderson RL, Ganter M. Development process for custom three-dimensional printing (3DP) material systems. *J Manuf Sci Eng* 2010;132:011008.
- [53] Bailey A, Merriman A, Elliott A, Basti M. Preliminary testing of nanoparticle effectiveness in binder jetting applications. 27th Annu. Int. Solid Free. Fabr. Symp. 2016:1069–77.
- [54] Elliott A, Alsalihi S, Merriman AL, Basti MM. Infiltration of nanoparticles into porous binder jet printed parts. *Am J Eng Appl Sci* 2016;9:128–33.
- [55] ExOne | metal 3D printers – direct material 3D metal printing. Available at: <https://www.exone.com/en-US/3D-printing-systems/metal-3d-printers>. [Accessed September 2019].
- [56] Miyajima H, Momenzadeh N, Yang L. Effect of printing speed on quality of printed parts in Binder Jetting Process. *Addit. Manuf.* 2018;20:1–10.
- [57] Hon KKB, Li L, Hutchings IM. Direct writing technology-Advances and developments. *CIRP Ann - Manuf Technol* 2008;57:601–20.
- [58] Hoey JM, Lutfurakhmanov A, Schulz DL, Akhatov IS. A review on aerosol-based direct-write and its applications for microelectronics. *J. Nanotechnol.* 2012;2012.
- [59] Rahman T, Renaud L, Heo D, Renn M, Panat R. Aerosol based direct-write micro-additive fabrication method for sub-mm 3D metal-dielectric structures. *J Micromech Microeng* 2015;25.
- [60] Khan S, Nguyen TP, Thiery L, Vairac P, Briand D. Aerosol jet printing of miniaturized, low power flexible micro-hotplates. *Proceedings* 2017;1:316.
- [61] Mahajan A, Frisbie CD, Francis LF. Optimization of aerosol jet printing for high-resolution , high- aspect ratio silver lines. *ACS Appl Mater Interfaces* 2013;5: 4856–64.
- [62] Kopola P, et al. Aerosol jet printed grid for ITO-free inverted organic solar cells. *Sol Energy Mater Sol Cells* 2012;107:252–8.
- [63] Jones CS, Lu X, Renn M, Stroder M, Shih WS. Aerosol-jet-printed, high-speed, flexible thin-film transistor made using single-walled carbon nanotube solution. *Microelectron Eng* 2010;87:434–7.
- [64] Wilkinson NJ, Smith MAA, Kay RW, Harris RA. A review of aerosol jet printing — a non-traditional hybrid process for micro-manufacturing. *Int J Adv Manuf Technol* 2019;105:4599–619. <https://doi.org/10.1007/s00170-019-03438-2>.
- [65] Kim N, Han KN. Future direction of direct writing. *J Appl Phys* 2010;102801.
- [66] Secor EB. Principles of aerosol jet printing. 2018.
- [67] Periasamy Ravindran E, Davis J. Multicomponent evaporation of single aerosol droplets. *J Colloid Interface Sci* 1982;85:278–88.
- [68] Widmann JF, Davis EJ. Evaporation of multicomponent droplets. *Aerosol Sci Technol* 1997;27:243–54.
- [69] Ha M, et al. Aerosol-jet-printed, 1 volt h-bridge drive circuit on plastic with integrated electrochromic pixel. *ACS Appl Mater Interfaces* 2013;5:13198–206.
- [70] Secor EB. Principles of aerosol jet printing. *Flex. Print. Electron.* 2018;3.
- [71] Hedges M, Marin AB, Hedges M. 3D aerosol jet ® printing - adding electronics functionality to RP/RM. 14–15. 2012.
- [72] 3D printed electronics - aerosol jet technology - optomec. Available at: <https://www.optomec.com/printed-electronics/aerosol-jet-technology/>. [Accessed July 2019].
- [73] Sadeq Saleh M, HamidVishkasougeh M, Zbib H, Panat R. Polycrystalline micropillars by a novel 3-D printing method and their behavior under compressive loads. *Scripta Mater* 2018;149:144–9.
- [74] Cai F, et al. High resolution aerosol jet printing ofD- band printed transmission lines on flexible LCP substrate characterize the DC performance of the printed metal. 2014. <https://doi.org/10.1109/MWSYM.2014.6848597>. 0–2.
- [75] Rahman T, Rahimi A, Gupta S, Panat R. Sensors and Actuators A : physical Microscale additive manufacturing and modeling of interdigitated capacitive touch sensors. *Sensor Actuator Phys* 2016;248:94–103.
- [76] Salary R, et al. Computational fluid dynamics modeling and online monitoring of aerosol jet printing process. *J. Manuf. Sci. Eng. Trans. ASME* 2017;139.
- [77] Secor EB. Guided ink and process design for aerosol jet printing based on annular drying effects. *Flex. Print. Electron.* 2018;3.
- [78] Lee G, et al. Aerodynamically focused nanoparticle (AFN) printing: novel direct printing technique of solvent-free and inorganic nanoparticles. *ACS Appl Mater Interfaces* 2014;6:16466–71.
- [79] Qi L, McMurry PH, Norris DJ, Girshick SL. Micropattern deposition of colloidal semiconductor nanocrystals by aerodynamic focusing. *Aerosol Sci Technol* 2010; 44:55–60.
- [80] Chen G, Gu Y, Tsang H, Hines DR, Das S. The effect of droplet sizes on overspray in aerosol-jet printing. *Adv Eng Mater* 2018;20.
- [81] Hoey JM, Akhatov IS, Swenson OF, S DL. Convergent-divergent-convergent nozzle focusing of aerosol particles for micron-scale direct writing. 2008.
- [82] Schulz DL, et al. Collimated aerosol beam deposition: sub-5- μm resolution of printed actives and passives. *IEEE Trans Adv Packag* 2010;33:421–7.
- [83] Blumenthal, T., Fratello, V., Nino, G. & Ritala, K. Aerosol Jet® printing onto 3D and flexible substrates.
- [84] Thomas JW. Gravity settling of particles in a horizontal tube. *J Air Pollut Contr Assoc* 1958;8:32–4.
- [85] Behera D, et al. Current challenges and potential directions towards precision microscale Additive manufacturing – Part IV: future perspectives. *Precis. Eng.* 2021;68:197–205. <https://doi.org/10.1016/j.precisioneng.2020.12.014>. In this issue.